

See discussions, stats, and author profiles for this publication at: <https://www.researchgate.net/publication/5650640>

# Synchrotron-Derived Vibrational Data Confirm Unprotonated Oxo Ligand in Myoglobin Compound II

ARTICLE *in* JOURNAL OF THE AMERICAN CHEMICAL SOCIETY · MARCH 2008

Impact Factor: 12.11 · DOI: 10.1021/ja077823+ · Source: PubMed

---

CITATIONS

22

---

READS

25

7 AUTHORS, INCLUDING:



Wolfgang Sturhahn

California Institute of Technology

330 PUBLICATIONS 5,328 CITATIONS

SEE PROFILE



Ercan E Alp

Argonne National Laboratory

394 PUBLICATIONS 5,302 CITATIONS

SEE PROFILE

## Synchrotron-Derived Vibrational Data Confirm Unprotonated Oxo Ligand in Myoglobin Compound II

Weiqiao Zeng,<sup>†</sup> Alexander Barabanschikov,<sup>†</sup> Yunbin Zhang,<sup>†</sup> Jiyong Zhao,<sup>‡</sup> Wolfgang Sturhahn,<sup>‡</sup> E. Ercan Alp,<sup>‡</sup> and J. Timothy Sage<sup>\*,†</sup>*Department of Physics and Center for Interdisciplinary Research on Complex Systems, Northeastern University, Boston, Massachusetts 02115, and Advanced Photon Source, Argonne National Laboratory, Argonne, Illinois 60439*

Received October 11, 2007; E-mail: jtsage@neu.edu

Cleavage of dioxygen bound to the iron atom of heme enzymes creates reactive monooxygenated heme species, denoted compounds I and II, having formal Fe(V) and Fe(IV) oxidation states. These are key intermediates in the reactive cycles of numerous enzymes including heme-copper oxidases, peroxidases, catalases, and cytochromes P-450.<sup>1</sup> Ferryl species of myoglobin (Mb) are formed during reperfusion of muscle tissue following ischemia, and their role in oxidative tissue damage is under active discussion.<sup>2</sup>

The protonation state of the oxo ligand in compound II has implications for the reactivity of this intermediate.<sup>3</sup> Standard methods lack direct sensitivity to the presence of the proton, and previous structural investigations have therefore used the length of the Fe–O bond as an indirect indication of the protonation state, which should affect the Fe–O bond order. Crystallographic investigations on ferryl intermediates of several heme proteins have identified Fe–O distances near 190 pm, suggesting a single bond to a protonated oxygen.<sup>3a,4</sup> On the other hand, EXAFS results have identified 170 pm Fe–O distances in proteins that have histidine bound trans to the oxygen, consistent with the traditional formulation as a double bond between the Fe and an unprotonated oxo group.<sup>5</sup> EXAFS investigations find a “long” Fe–O bond only for compound II of chloroperoxidase, which has a trans cysteine thiolate ligand.<sup>5b</sup>

In order to address this issue, we seek more direct vibrational signatures for protonation of the monooxygen ligand. Figure 1 compares the vibrational dynamics of the heme Fe in Mb compound II [Mb(IV)=O] with those observed for hydroxymetMb [Mb(III)–OH], which is well established to have a hydroxyl ion bound to the ferric heme iron. Both spectra are recorded using nuclear resonance vibrational spectroscopy (NRVS),<sup>6</sup> which reveals Fe–ligand vibrations as sidebands on the 14.4 keV nuclear resonance of <sup>57</sup>Fe. The flux density (approximately 10<sup>9</sup> photons/s dispersed over a 5 × 0.5 mm<sup>2</sup> area) is significantly lower than in other X-ray-based structural methods, and we observe no time-dependent structural changes attributable to radiation damage at the 20–30 K temperatures of our measurements.

The Fe–O stretching vibrations appear at 805 and 556 cm<sup>−1</sup>. Both are spectrally isolated from other vibrations, in contrast with resonance Raman measurements, where <sup>16</sup>O/<sup>18</sup>O difference spectra distinguish these vibrations from neighboring vibrations of the heme macrocycle.<sup>3c,7</sup> The 250 cm<sup>−1</sup> frequency increase indicates a substantially stronger Fe–O bond in Mb(IV)=O than in Mb(III)–OH, consistent with an unprotonated oxygen for the former complex. Comparison with DFT predictions of the vibrational densities of states (VDOS), presented in Figure 2, confirms the identification of these vibrations and further associates a 250 cm<sup>−1</sup> frequency increase for Mb(IV)=O with a 17 pm decrease in bond

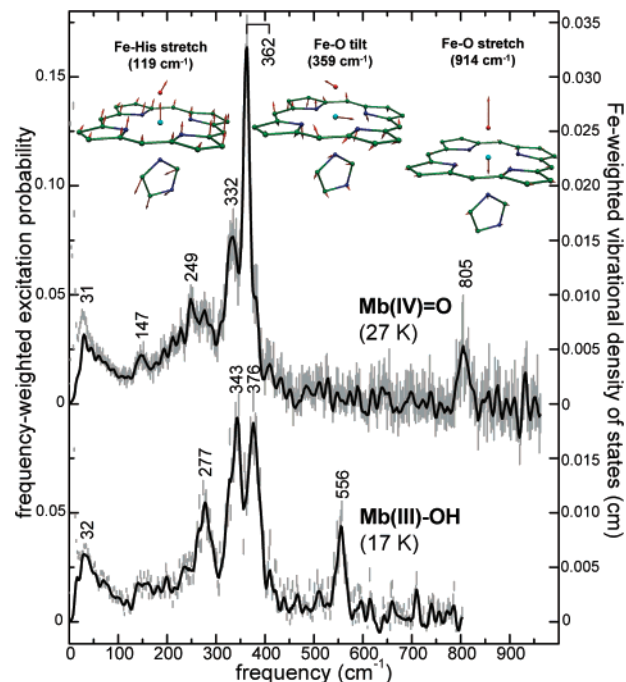


**Figure 1.** Vibrational dynamics of the heme Fe reveal an unprotonated oxo ligand in Mb(IV)=O, in contrast with the bound hydroxyl group in Mb(III)–OH. Protonation of the oxo ligand results in a downshift of the Fe–O stretching frequency from 805 cm<sup>−1</sup> to 556 cm<sup>−1</sup>, and splits the Fe–O tilting vibrations, which are degenerate near 362 cm<sup>−1</sup> in Mb(IV)=O, but are separated by 33 cm<sup>−1</sup> in the asymmetrically protonated heme Mb(III)–OH complex. Error bars represent the normalized experimental signal, multiplied by frequency to facilitate comparison with the extracted vibrational density of states, presented as a solid curve. Normal mode representations show only the heme core.

length. Absolute values of the predicted frequencies and bond lengths are somewhat larger and smaller, respectively, than the observed values, possibly due in part to the absence of hydrogen bonds to the oxygen ligand in the calculated structures.

The calculations further identify the dominant spectral features observed near 360 cm<sup>−1</sup> in both complexes with tilting of the Fe–O bond with respect to the heme plane, coupled with stretching of the Fe–N bonds to the heme. Protonation lifts the degeneracy of these vibrations in either oxidation state, with Fe–O tilting parallel to the FeOH plane predicted at higher frequency than tilting perpendicular to this plane. These frequencies are unresolved in Mb(IV)=O but are separated by 30 cm<sup>−1</sup> in both protonated complexes. Interestingly, calculations predict that oxidation of Mb(III)–OH creates spin density on the porphyrin and one propionate, with minimal influence on the immediate Fe environment. As a result, vibrational (Figure 2, center panel) and structural predictions for Mb(IV)–OH strongly resemble those for Mb(III)–OH, sug-

<sup>†</sup> Northeastern University.<sup>‡</sup> Argonne National Laboratory.

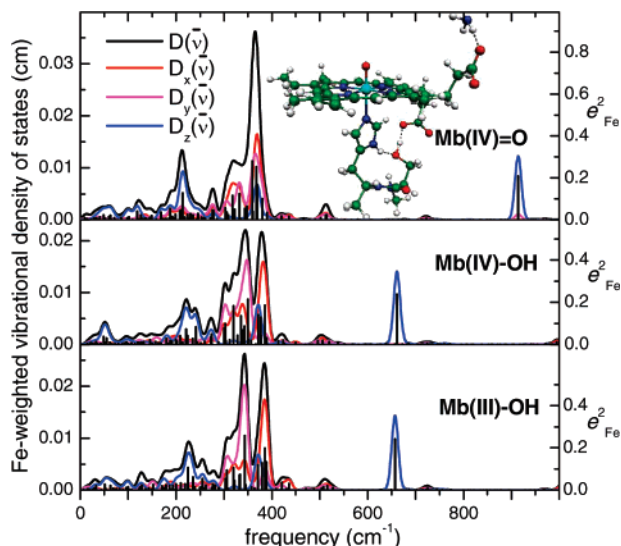


**Figure 2.** Predicted vibrational densities of states for models of the Mb(IV)=O, Mb(IV)-OH, and Mb(III)-OH active sites reveal a 35–40 cm<sup>-1</sup> splitting of the major feature due to Fe–O tilting in the two protonated species. The predicted 250 cm<sup>-1</sup> downshift of the Fe–O stretching frequency reflects the reduced Fe–O bond order upon protonation of the oxygen. Black bars indicate the areas contributed by individual modes, and colors represent the direction of Fe motion in an orthogonal coordinate system with the *z*-axis oriented normal to the mean plane of the four pyrrole nitrogen atoms and the *x*-axis connecting two opposite pyrrole nitrogens, nearly parallel to the imidazole and FeOH planes. DFT calculations used *Gaussian03*<sup>13a</sup> with the B3LYP functional<sup>13b,c</sup> on a model including the full protoporphyrin IX, the monooxygen ligand, and the Ser 92 and His 93 amino acids. The basis was Ahlrich's VTZ<sup>13d</sup> for Fe and 6-31G\* for all other atoms.

gesting that Mb(III)-OH provides a reliable vibrational model for the putative protonated Mb(IV)-OH.

The Fe–His vibration predicted to appear at 119 cm<sup>-1</sup> may correspond to the feature resolved near 147 cm<sup>-1</sup> in Mb(IV)=O. Imidazole ring translation dominates the predicted mode character, accounting for the modest Fe signal. The reduced frequency in comparison with the 220–230 cm<sup>-1</sup> frequency observed for deoxyMb<sup>6a,8</sup> is consistent with the increased Fe–His bond length observed for low spin hemes, and suggests that this frequency may be a sensitive probe of the Fe–His bond in future studies. Fe–His and Fe–pyrrole bond stretching may both contribute to the congested 250–300 cm<sup>-1</sup> region.

Structural models derived from X-ray crystallography have long Fe–O bonds that have been attributed to a protonated oxo ligand.<sup>3a,4</sup> However, contributions from multiple spectroscopically distinct species<sup>9</sup> complicate the structural interpretation of X-ray diffraction data. Absorption measurements recorded on Mb crystals before exposure to peroxide reveal evidence for low-spin contributions,<sup>9</sup> which might result in part from displacement of the heme water ligand by ammonia present in the concentrated ammonium sulfate crystallization solutions.<sup>10</sup> Additional spectroscopic changes are observed following reaction with peroxide and exposure to the X-ray doses used for structural determination.<sup>9</sup> Although some of the resulting species remain to be identified, our calculations (Figure 2) suggest that the Mb(III)-OH likely to result from reduction of Mb(IV)=O under sustained intense X-irradiation would be indistinguishable from Mb(IV)-OH. Moreover, possible contributing species have heme ligands nearly isoelectronic with the oxo group, but with Fe–ligand bonds ranging up to 213 pm in length, if some heme sites are reduced to the ferrous state.<sup>11</sup> As a result, the 190 pm Fe–O bond length in the structural model has limited value as an indicator of the protonation state of the heme-bound oxo group.

In contrast, the frequency separation of the Fe–O tilting modes in Mb(III)-OH directly reflects the asymmetric protonation of the oxygen ligand, and the observed degeneracy of these modes in Mb(IV)=O confirms the ligation of an unprotonated oxo group to the Fe. We believe that this spectroscopic approach will extend to analogous states of other histidine-ligated heme proteins. Our experimental and computational results establish the high sensitivity of the Fe–O stretching frequency, commonly observed with conventional techniques, to the decreased Fe–O bond order upon protonation and support interpretation of the 565 cm<sup>-1</sup> Fe–O frequency observed for compound II of the thiolate-ligated heme in chloroperoxidase as indicative of a protonated oxo group.<sup>12</sup> Together, Fe–O stretching and FeO tilting will provide distinctive vibrational signatures for the protonation state in continuing structural investigations of ferryl heme protein intermediates.

**Acknowledgment.** We acknowledge financial support from the National Science Foundation (PHY-0545787). Use of the Advanced Photon Source was supported by the U.S. Department of Energy, Basic Energy Sciences, Office of Science, under Contract No. DE-AC02-06CH11357. We thank Nathan Silvermail, Dr. Bogdan Leu, Dr. Chuanjian Hu, and Prof. W. Robert Scheidt for assistance during NRVS data collection.

**Supporting Information Available:** Sample preparation, experimental and computational procedures, optimized structures and spin densities, selected structural parameters, Raman data, and animations of iron–ligand vibrations. Complete ref 13a. This material is available free of charge via the Internet at <http://pubs.acs.org>.

## References

- (1) (a) Sono, M.; Roach, M. P.; Coulter, E. D.; Dawson, J. H. *Chem. Rev.* **1996**, *96*, 2841–2887. (b) Denisov, I. G.; Makris, T. M.; Sligar, S. G.; Schlichting, I. *Chem. Rev.* **2005**, *105*, 2253–2277. (c) Meunier, B.; de Visser, S. P.; Shaik, S. *Chem. Rev.* **2004**, *104*, 3947–3980.
- (2) (a) Reeder, B. J.; Wilson, M. T. *Curr. Med. Chem.* **2005**, *12*, 2741–2751. (b) Flögel, U.; Godecke, A.; Klotz, L. O.; Schrader, J. *FASEB J.* **2004**, *18*, 1156–1158.
- (3) (a) Hersleth, H.-P.; Ryde, U.; Rydberg, P.; Gorbitz, C. H.; Andersson, K. K. *J. Inorg. Biochem.* **2006**, *100*, 460–476. (b) Behan, R. K.; Green, M. T. *J. Inorg. Biochem.* **2006**, *100*, 448–459. (c) Terner, J.; Palaniappan, V.; Gold, A.; Weiss, R.; Fitzgerald, M. M.; Sullivan, A. M.; Hosten, C. M. *J. Inorg. Biochem.* **2006**, *100*, 480–501.
- (4) (a) Berglund, G. I.; Carlsson, G. H.; Smith, A. T.; Szöke, H.; Henriksen, A.; Hajdu, J. *Nature* **2002**, *417*, 463–468. (b) Bonagura, C. A.; Bhaskar, B.; Shimizu, H.; Li, H.; Sundaramoorthy, M.; McRee, D. E.; Goodin, D. B.; Poulos, T. L. *Biochemistry* **2006**, *42*, 19, 5600–5608.
- (5) (a) Chance, M.; Powers, L.; Kumar, C.; Chance, B. *Biochemistry* **1986**, *25*, 1259–1265. (b) Green, M. T.; Dawson, J. H.; Gray, H. B. *Science* **2004**, *304*, 1653.
- (6) (a) Sage, J. T.; Durbin, S. M.; Sturhahn, W.; Wharton, D. C.; Champion, P. M.; Hession, P.; Sutter, J.; Alp, E. E. *Phys. Rev. Lett.* **2001**, *86*, 4966–4969. (b) Zeng, W.; Silvermail, N. J.; Wharton, D. C.; Georgiev, G. Y.; Leu, B. M.; Scheidt, W. R.; Zhao, J.; Sturhahn, W.; Alp, E. E.; Sage, J. T. *J. Am. Chem. Soc.* **2005**, *127*, 11200–11201.
- (7) Feis, A.; Marzocchi, M. P.; Paoli, M.; Smulevich, G. *Biochemistry* **1994**, *33*, 4577–4583.
- (8) Argade, P. V.; Sassaroli, M.; Rousseau, D. L.; Inubushi, T.; Ikeda-Saito, M.; Lapidot, A. *J. Am. Chem. Soc.* **1984**, *106*, 6593–6596.
- (9) Hersleth, H.-P.; Uchida, T.; Röhr, A. K.; Teschner, T.; Schünemann, V.; Kitagawa, T.; Trautwein, A. X.; Gorbitz, C. H.; Andersson, K. K. *J. Biol. Chem.* **2007**, *282*, 23372–23386.
- (10) Zhu, L.; Sage, J. T.; Champion, P. M. *Biochemistry* **1993**, *32*, 11181–11185.
- (11) Engler, N.; Ostermann, A.; Gassmann, A.; Lamb, D. C.; Prusakov, V. E.; Schott, J.; Schweitzer-Stenner, R.; Parak, F. G. *Biophys. J.* **2000**, *78*, 2081–2092.
- (12) Stone, K. L.; Behan, K.; Green, M. T. *Proc. Natl. Acad. Sci. U.S.A.* **2006**, *103*, 12307–12310.
- (13) (a) Frisch, M. J.; et al. *Gaussian 03*, revision C.01; Gaussian Inc.: Wallingford, CT, 2004 (full ref is in the SI). (b) Becke, A. D. *J. Chem. Phys.* **1993**, *98*, 5648–5652. (c) Lee, C.; Yang, W.; Parr, R. G. *Phys. Rev. B* **1988**, *37*, 785–789. (d) Schäfer, A.; Horn, H.; Ahlrichs, R. *J. Chem. Phys.* **1992**, *97*, 2571.

JA077823+